

**AIAA-82-0887**

**Surface Hardness Distribution Effects Upon  
Contact, Gap and Joint Conductances**

M.M. Yovanovich, A.H. Hegazy and  
J. DeVaal, Univ. of Waterloo, Ontario, Canada



**AIAA/ASME 3rd Joint Thermophysics,  
Fluids, Plasma and Heat Transfer  
Conference**

June 7-11, 1982/St. Louis, Missouri

SURFACE HARDNESS DISTRIBUTION EFFECTS  
UPON CONTACT, GAP AND JOINT CONDUCTANCES

M.M. Yovanovich\*, A.H. Hegazy\*\* and J. DeVaal†  
Thermal Engineering Group  
Department of Mechanical Engineering  
University of Waterloo  
Waterloo, Ontario N2L 3G1

Abstract

Dimensionless conductance correlations are developed for work hardened rough surfaces. Both integral and integrated geometric-mechanical models are considered. The integrated model yields a lower bound while the conventional bulk hardness model yields the upper bound on the contact conductance. The iterated model conductances lie between these bounds. Results of the analyses are presented in graphical form. The proposed correlations are in good quantitative agreement with limited empirical data.

Greek Symbols

$\alpha, \alpha_1, \alpha_2$  = accommodation parameter and accommodation coefficients for solids 1 and 2  
 $\beta$  =  $(2\gamma/\gamma+1)/Pr$  gas parameter  
 $\gamma$  =  $C_p/C_v$  specific heat ratio  
 $\zeta$  = factor between 4 and 6  
 $\lambda, \lambda_0$  = molecular mean free path  
 $\sigma, \sigma_1, \sigma_2$  = effective surface roughness and surface roughnesses of solids 1 and 2

Nomenclature

$A_a, A_r$  = apparent and real contact areas  
 $a$  = mean contact spot radius  
 BH = Brinell hardness number  
 BHM = bulk hardness model  
 $C_1, C_2, C_3$  = constants  
 $C$  =  $\frac{ch}{k_s}$  dimensionless contact conductance  
 $C_c, C_g, C_j$  = contact, gap and joint dimensionless conductances  
 $F$  = contact force  
 $H$  = hardness  
 $H_b, H_{eff}, H_{max}$  = bulk, effective, and maximum hardness  
 $h_c, h_g, h_j$  = contact, gap and joint conductances  
 INM = integral hardness model  
 ITM = iterative hardness model  
 $K$  =  $k_{go}/k_s$  conductivity ratio  
 $k_1, k_2$  = conductivity of the contacting solids  
 $k_g, k_{go}, k_s$  = gap, gas and harmonic mean conductivities  
 $M$  =  $\alpha\beta A/\sigma$  gas parameter  
 $m$  = mean absolute surface slope  
 $P, P_g, P_{go}$  = apparent contact pressure, gas pressure and reference gas pressure  
 $Pr$  =  $\mu C_p/k_g$  Prandtl number  
 RH = Rockwell hardness number  
 $T, T_0$  = gap and reference temperature  
 $t$  = depth of penetration  
 $t_b, t_0$  = depth of penetration at bulk and maximum hardness  
 VH = Vickers hardness number  
 $Y$  = separation between the surfaces  
 $Y_0$  = separation between the surfaces at zero load

Introduction

During the past three decades considerable attention has been given to the problem of conforming rough surfaces. A striking feature of the published experimental and analytical results due to several investigators has been the very wide discrepancies of these results using nominally similar materials. The question arises whether these discrepancies are due to the experimental procedure or due to the geometric, thermal or physical properties of the contacting surfaces which appear in the models.

Boeschoten and Van der Held<sup>1</sup>, in one of the earlier experimental and analytical works on thermal conductance between aluminum and other metals, reported that the micro-hardness measurements of aluminum rods gave a value seven times larger than the hardness values found in the literature. They attributed this to the drawing of the rods. In their analysis they used the larger value.

Laming<sup>2</sup> considered the effect of hardness variation in his thermal model. From his thermal conductance measurements and following Mott's<sup>3</sup> analysis he was able to determine the form of the hardness variation for his specimens. He claimed that the hardness value is very important in correlating thermal conductance data.

Clausing and Chao<sup>4</sup> measured micro-hardness variations in several metals which were used in their experimental work. They reported these hardness values but did not attempt to incorporate them in their model.

Henry<sup>5</sup> made micro-hardness measurements on stainless steel type 416. These values as well as the results of Vickers and Knoop tests are reported in Fig. 1. The author concluded that a considerable scatter is indicated, but a definite trend is observed, i.e., the hardness decreases with increasing indentation size or with increasing depth of penetration.

The purpose of this paper is to develop a model incorporating hardness variation and to show its effect on the prediction of contact, gap and joint conductance.

\*Professor, Associate Fellow AIAA  
 \*\*Graduate Research Assistant  
 †Graduate Research Assistant

### Hardness Measurements and Distribution

Hardness measurements have been made for Nickel 200<sup>8</sup> and stainless steel 304<sup>9</sup>. The Vickers, Rockwell and Brinell test results are shown in Figs. 2 and 3. These figures represent the measured hardness values versus depth of penetration. It is clear that hardness decreases with increasing depth of penetration. From the measurements the hardness distribution can be expressed in terms of the depth of penetration by the following equations:

$$\begin{aligned}
 H &= H_{\max} = \text{const.} & t &\leq t_0 \\
 H &= H(t) = c_1 t^{c_2} + c_3 & t_0 &\leq t \leq t_b \quad (1) \\
 H &= H_b = \text{const.} & t &\geq t_b
 \end{aligned}$$

where  $t_b$  is the depth of the work-hardened layer which will vary depending upon the machining process and type of material.

According to Kragelskii<sup>6</sup> the high micro-hardness values in these layers can be explained by the fact that in this region the material is subjected to maximum work-hardening.

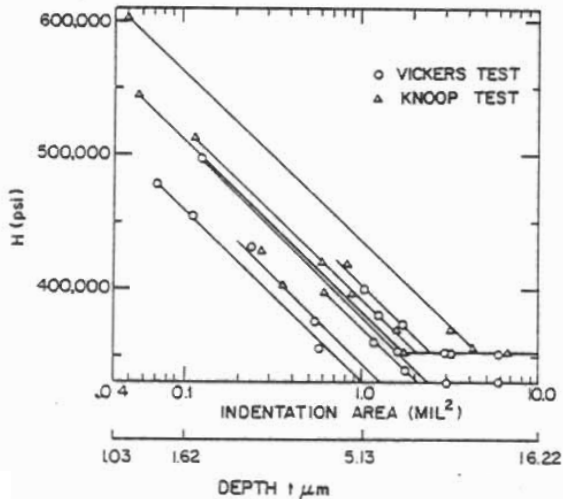


Fig. 1 Hardness of stainless steel type 416 Ref.5.

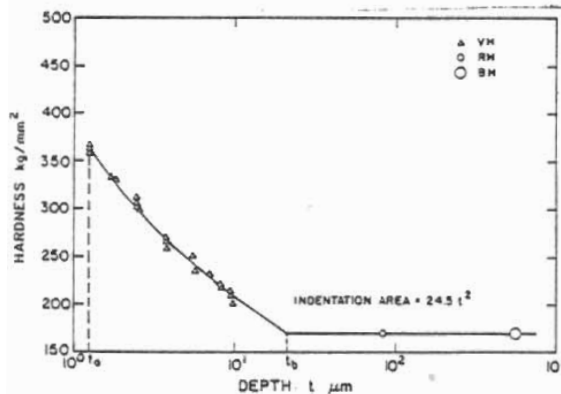


Fig. 2 Hardness of Nickel 200 Ref. 8.

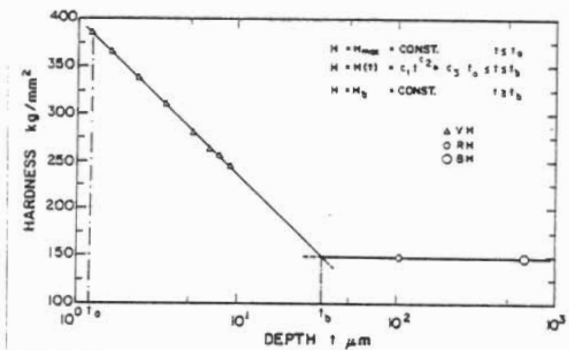


Fig. 3 Hardness of Stainless steel 304 Ref. 9.

### Effect of Hardness Distributions on Thermal Conductance Correlations

Two models are proposed to handle the effect of hardness distribution. These two models use contact, gap and joint conductance correlations developed by Yovanovich<sup>10</sup>.

The following models are based upon the usual assumptions<sup>10</sup> as well as the following:

- 1) One of the two contacting surfaces is smooth and has a constant hardness.
- 2) The second surface is rough and has a variable hardness, as given by Eq. (1), but the highest value is less than the hardness of the first one, i.e., surface 2 is softer than surface 1.

#### I. Iterative Hardness Model

For this model we assume that:

- 1) The asperity hardness depends on its location from the line of highest peaks which is the line of contact at zero load, Fig. 4.
- 2) The hardness of the highest peaks is equal to  $H_{2\max}$ .
- 3) The separation at zero load  $Y_0$  is the distance between the surface mean plane and the line of highest peaks and is given by

$$Y_0 = \zeta \sigma \quad (2)$$

where  $\zeta$  is a factor between 4 and 6.

The basic idea in this model is to determine the location of the contact line and the corresponding hardness under a certain contact pressure.

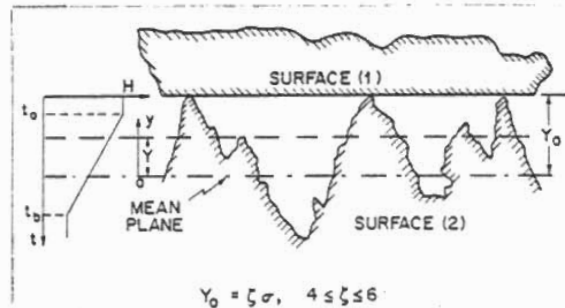


Fig. 4 Schematic diagram of a rough surface with a hardness layer in contact with an ideal flat surface

### Solution Procedure

Consider two surfaces in contact under a nominal pressure  $P$  for which we are interested in predicting the contact, gap and joint conductance. The two surfaces satisfy the previous assumptions. Knowing surface 2 roughness and choosing a proper value of  $\zeta$ , the separation at zero load can be calculated.

An initial guess is needed for the hardness and the corresponding depth  $t$  to begin the iterative procedure. They are taken as

$$H = H_{2max} \quad (3)$$

$$t = t_0 \quad (4)$$

Knowing the surface 2 RMS roughness  $\sigma$ , nominal pressure  $P$  and the initial hardness guess, the first approximation for the separation  $Y$  is computed by means of the following expression<sup>10</sup>:

$$Y = 1.184\sigma(-\ln[3.132P/H])^{0.547} \quad (5)$$

Having the first initial value of the separation, a new value of depth  $t$ , as shown in Fig. 4, is calculated as

$$t_{new} = Y_0 - Y \quad (6)$$

and the corresponding value of hardness is calculated from Eq. (1).

Now, a second approximation of depth and hardness is obtained. This cycle of depth and hardness iterations is continued until a relative convergence criterion is satisfied, such as

$$\left| \frac{t_{new} - t_{old}}{t_{new}} \right| < \text{Tolerance} \quad (7)$$

The final value of hardness is then used to calculate the contact conductance using Yovanovich correlation<sup>10</sup> which is:

$$C_c = \frac{ch_c}{k_s} = 1.25 m (P/H)^{0.95} \quad (8)$$

and the gap conductance, from [10], is

$$C_g = \frac{ch_g}{K_s} = \frac{K}{(Y/\sigma) + M} \quad (9)$$

where  $Y/\sigma$  is defined by Eq.(5),  $K$  is the conductivity ratio and  $M$  is a gas parameter defined by:

$$M = \alpha \delta \frac{A_0}{\sigma} \left( \frac{T}{T_0} \right) \left( \frac{P_g}{P_g} \right) \quad (10)$$

Knowing the contact and gap conductance, the total or joint conductance  $C_j$  is equal to the sum of the two, or

$$C_j = C_c + C_g \quad (11)$$

A flow chart of the solution procedure is shown in Fig. 5. Not all of the sophistication of the original procedure has been included, but the essentials are present.

### II. Integral Hardness Model

#### Discussion of Hardness Models

An inherent assumption in the development of

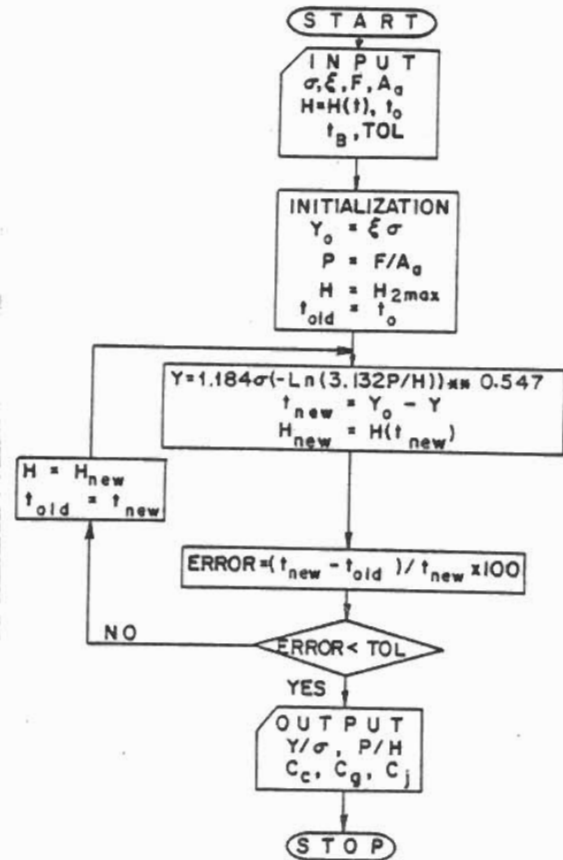


Fig. 5 Iterative model flow chart.

the iterative model, discussed previously, is the requirement that the hardness of higher asperities be greater than that of asperities having lower heights. This idea has justification if one realizes that, during the creation of the surface, the highest asperities were formed from material which was displaced the greatest distance from the original surface and, through the roughness forming process, has been work hardened the most. A situation of this nature could exist in very rough, highly worked surfaces, e.g., surfaces bead blasted with very large beads under a high pressure application.

A model is proposed where the hardness at any depth in the rough surface is simply a function of the local depth of penetration below the surface at that point (Fig. 6). The model which most closely approximates this condition is given by assuming that each asperity has the same hardness variation as the original measured variation.

In the case of low slopes on the rough surface, assigning a hardness variation to the asperity will be seen to approximate the condition of hardness variation following the surface such that the hardness versus local depth of penetration condition is preserved. This model is thought to better

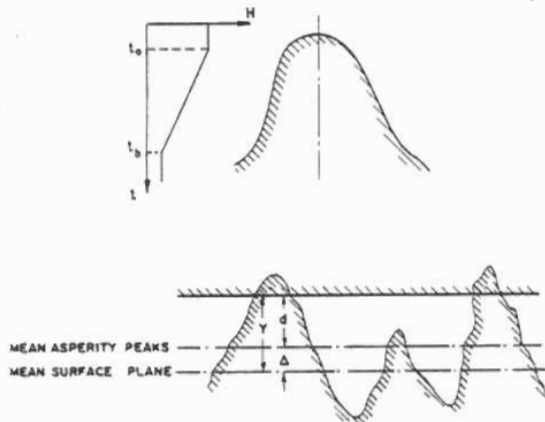


Fig. 6 Schematic diagram for INM and asperity hardness distribution.

describe surfaces which are not extremely rough and do not have high slopes. The model also has the advantage of not requiring an arbitrary datum locating the zero load, maximum hardness position in the rough surface, a condition which the previous model needed.

Analysis

Consider the contact between a rough and smooth surface having the properties defined previously. Using the method proposed by Greenwood and Williamson<sup>7</sup> we begin by defining the probability that an asperity exists between  $z$  and  $z + dz$  by  $\phi(z)dz$ .

The probability of making contact at any given asperity, having height  $z$ , is:

$$\text{prob}(z > d) = \int_d^{\infty} \phi(z)dz \quad (12)$$

Letting  $n$  be the surface density of asperities and  $A_a$  the nominal contact area gives the expected number of contacts as:

$$n = nA_a \int_d^{\infty} \phi(z)dz \quad (13)$$

Given the area in contact for a single asperity  $A_{ri}$  in terms of the compliance,  $w = z-d$ :

$$A_{ri} = 2\pi\beta w \quad (14)$$

where  $\beta$  is asperity tip radius.

The relation for the total area in contact is

given by:

$$A_r = 2\pi\beta n A_a \int_d^{\infty} (z-d)\phi(z)dz \quad (15)$$

A force balance on the real and apparent contact areas in terms of hardness gives

$$\frac{A_r}{A_a} = \frac{P}{H} \quad (16)$$

The total force on the contact is given by

$$F = PA_a = A_r H \quad (17)$$

substituting Eq. (15) into (17) yields

$$F = 2\pi\beta n A_a \int_d^{\infty} (z-d)H(z-d)\phi(z)dz \quad (18)$$

Defining the effective hardness as

$$H_{eff} = F/A_r \quad (19)$$

from Eq. (18) we can write

$$H_{eff} = \frac{\int_d^{\infty} (z-d)H(z-d)\phi(z)dz}{\int_d^{\infty} (z-d)\phi(z)dz} \quad (20)$$

where

$$H(z-d) = c_1(z-d)^{c_2} + c_3 \quad (21)$$

Results and Discussion

To demonstrate the effect of hardness distribution upon predicting contact, gap and joint conductance the following case is considered:

- a) Surface 1 is smooth and has a constant hardness  $H_1 > H_{2max}$ .
- b) Surface 2 is rough, of stainless steel 304, and has the hardness distribution shown in Fig. 3 and given by Eq. (1) with the following constants:

$c_1 = 3049.6$	$t_0 = 1.2 \mu m$
$c_2 = -0.024$	$t_b = 34 \mu m$
$c_3 = -2649.8$	$H_{2max} = 385 \text{ kg/mm}^2$
	$H_b = 150 \text{ kg/mm}^2$

- c) For the iterative model  $Y_0 = \zeta\sigma$  and  $\zeta = 4, 5$  and  $6$ .
- d) The interstitial fluid is air at  $17^\circ C$  and atmospheric pressure.

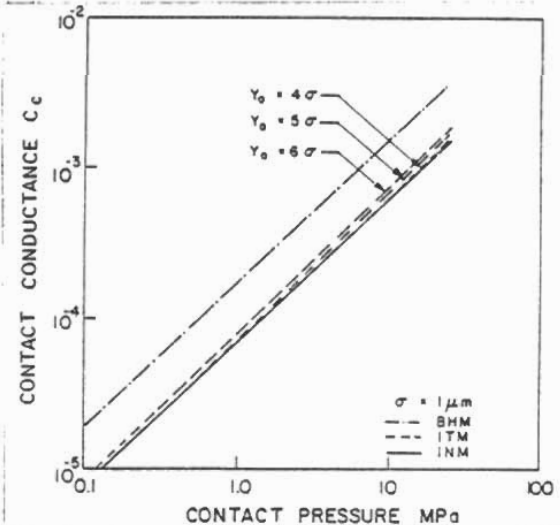


Fig. 7 Contact conductance for stainless steel 304 vs. apparent contact pressure for  $\sigma = 1 \mu m$

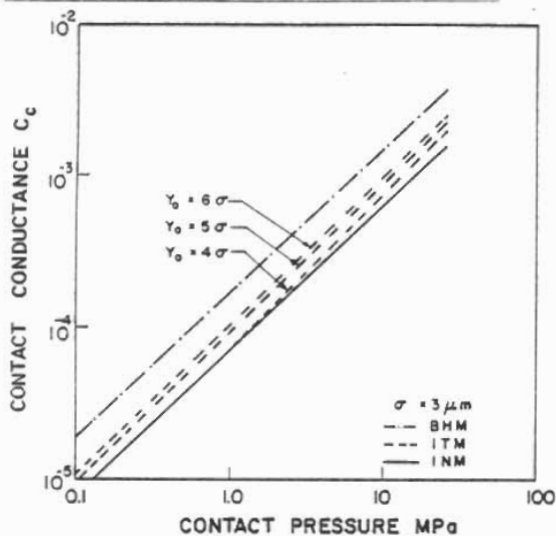


Fig. 8 Contact conductance for stainless steel 304 vs. apparent contact pressure for  $\sigma = 3 \mu\text{m}$ .

The results obtained by using the iterative and integral hardness models for  $\sigma = 1, 3$  and  $5 \mu\text{m}$  along with the bulk hardness model using the Yovanovich correlations<sup>10</sup> are given in Figures 7 through 15.

It is clear from these figures that the bulk hardness model (BHM) represents the upper limit while the integral hardness model (INM) represents the lower limit. Also these figures show how much the prediction by means of the ITM depends on the location of the surface mean plane, i.e., the separation at zero contact pressure. In general,

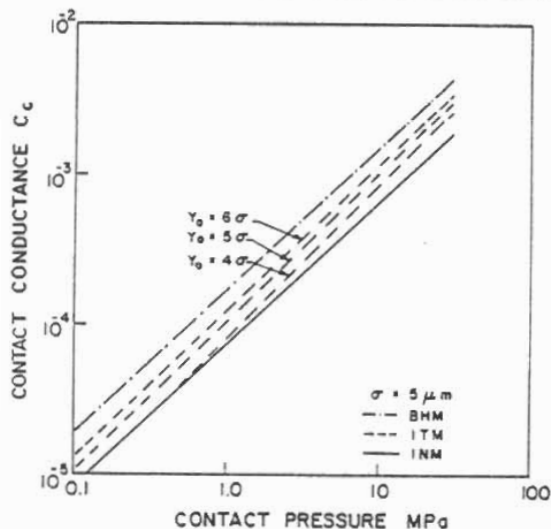


Fig. 9 Contact conductance for stainless steel 304 vs. apparent contact pressure for  $\sigma = 5 \mu\text{m}$ .

the values from the ITM lie between the values from the INM and BHM. Figures 7-9 show that as the RMS roughness increases the values of contact conductance from the ITM approach those of the BHM. It is also clear that the effect of hardness variation is important upon predicting the contact conductance. Figures 10-12 show the effect of hardness variation on predicting gap conductance, but in general, the difference between the three models is small especially at low contact pressure. Figures 13-15 show the variation of joint conductance with contact pressure for different values of RMS roughness using the three models. It is clear from these figures that the effect of hardness variation is still small at low contact pressure because the fluid conductance is predominant, but as the contact pressure increases the effect of hardness variation becomes significant.

#### Comparison Between Theory and Experiment

The predicted values of contact conductance based upon the two models presented in this paper are compared with the experimental results of Antonetti<sup>8</sup>. Antonetti measured the contact conductance of two Nickel 200 specimens having a hardness distribution shown in Fig. 2. The maximum value of  $362.3 \text{ kg/mm}^2$  occurred at a depth  $t_0 = 1.24 \mu\text{m}$  and the bulk value of  $170.4 \text{ kg/mm}^2$  was observed for  $t > t_b = 21.6 \mu\text{m}$ .

The hardness distribution between  $t_0$  and  $t_b$  can be described by

$$H(t) = 377.3t^{-0.2737} + 7.795 \quad (22)$$

The two cylindrical specimens have the following RMS roughness and mean asperity slope:

$$\begin{aligned} \sigma_1 &= 0.16 \mu\text{m} & m_1 &= 0.025 \\ \sigma_2 &= 4.29 \mu\text{m} & m_2 &= 0.239 \end{aligned}$$

Therefore, the effective surface roughness and slope are  $\sigma = 4.29 \mu\text{m}$  and  $m = 0.240$ .

The interface mean temperature ranged from  $97.4$  to  $117.8^\circ\text{C}$  while the nominal contact pressure ranged from  $698$  to  $3636 \text{ KN/m}^2$ .

The harmonic mean thermal conductivity was  $63.5 \text{ W/mK}$ . All measurements were obtained in a vacuum of approximately  $10^{-5} \text{ mm Hg}$ .

The predicted and measured values of dimensionless contact conductance are shown in Fig. 16 and tabulated in Table 1. From the figure it is clear that there is very good agreement between the ITM and the data for  $\zeta = 4$ . Table 1 also shows the location of the contact line and the corresponding hardness. It can be seen that the contact line ranged from approximately  $2.1$  to  $4.4 \mu\text{m}$  while the corresponding hardness ranged from approximately  $314$  to  $260 \text{ kg/mm}^2$ . The average contact hardness was approximately  $280 \text{ kg/mm}^2$ . Table 1 also shows the comparison between the theoretical and experimental values of the dimensionless contact conductances. It is seen that the percent difference lies between  $-10.9$  and  $14.4$ . The sum of the percent differences is  $1.38$  and the average percent difference is  $0.20$ .

#### Direct Approximate Method for Predicting Thermal Conductances

We present next an alternate direct method

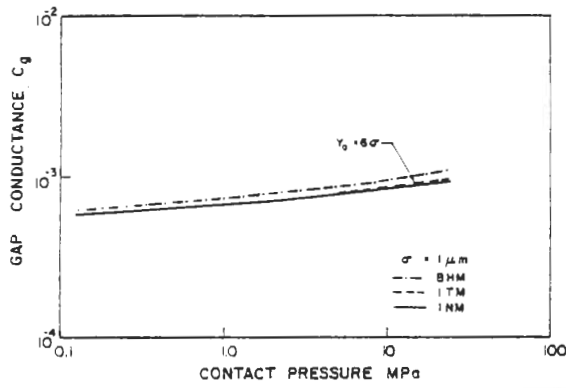


Fig. 10 Gap conductance when air is present for stainless steel 304 vs. apparent contact pressure for  $\sigma = 1\mu\text{m}$ .

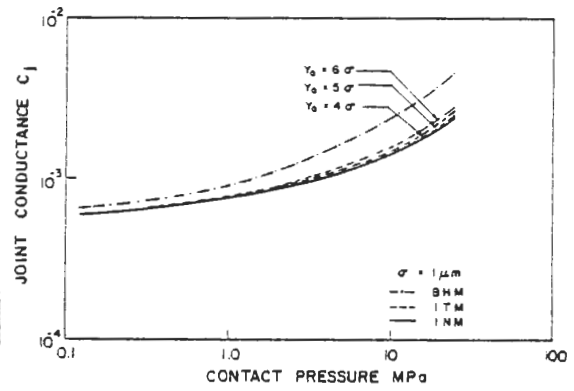


Fig. 13 Joint conductance in atmospheric air for stainless steel 304 vs. apparent contact pressure for  $\sigma = 1\mu\text{m}$ .

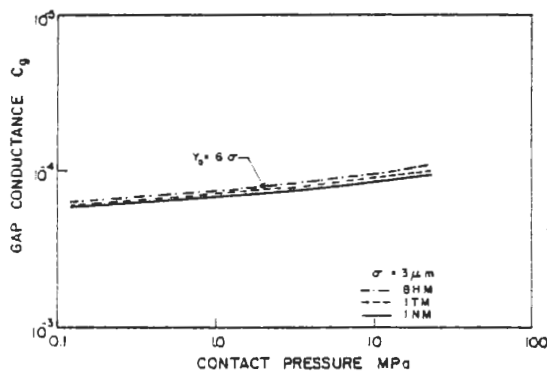


Fig. 11 Gap conductance when air is present for stainless steel 304 vs. apparent contact pressure for  $\sigma = 3\mu\text{m}$ .

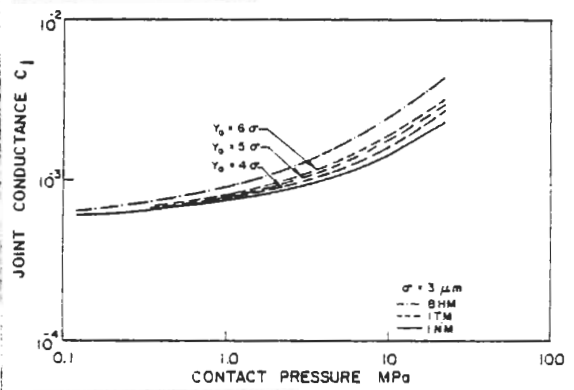


Fig. 14 Joint conductance in atmospheric air for stainless steel 304 vs. apparent contact pressure for  $\sigma = 3\mu\text{m}$ .

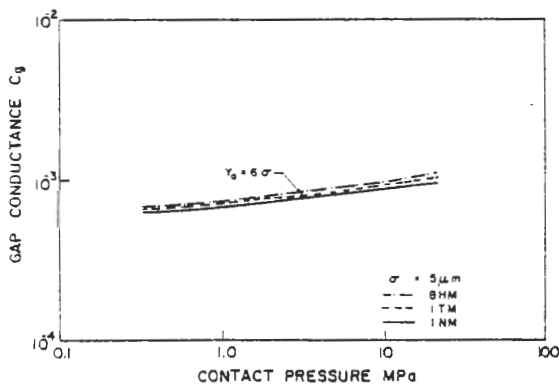


Fig. 12 Gap conductance when air is present for stainless steel 304 vs. apparent contact pressure for  $\sigma = 5\mu\text{m}$ .

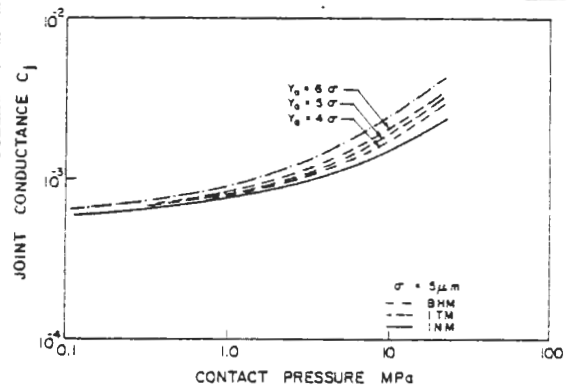


Fig. 15 Joint conductance in atmospheric air for stainless steel 304 vs. apparent contact pressure for  $\sigma = 5\mu\text{m}$ .

based upon the Yovanovich correlations<sup>10</sup> for determining the contact, gap and joint conductance for the thermal analyst who requires a fast, reliable technique for obtaining approximate values. The method is applicable for systems which operate within a limited range of contact pressures. The basic idea is to use an effective hardness value corresponding to an indentation area equal to the average area of a single contact spot resulting from the mean contact pressure defined by the minimum and maximum pressures. The complete solution procedure is given in Fig. 17.

This procedure was examined using the experimental results of Antonetti<sup>8</sup>. For his mean contact pressure of 2167 KN/m<sup>2</sup>, an effective hardness value of 300 kg/mm<sup>2</sup> was computed. Using this hardness value in the BHM of Yovanovich<sup>10</sup>, good agreement between theory and experiment is seen in Fig. 18. The percent difference ranged from -1.2 up to 15.1 with an average percent difference of 7.1.

Based upon this example we can say that the BHM will give a good engineering estimate of the contact conductance in a limited range of contact pressure.

#### Conclusions and Recommendations

Dimensionless contact, gap and joint conductances have been developed incorporating surface hardness distributions. Iterated and integral geometric-mechanical models have been considered.

The conventional mechanical model assuming uniform hardness equal to the bulk value (BHM) yields the upper bound on the conductances, while the integrated hardness model (INM) yields the lower bound on the conductances. The iterated hardness model (ITM) conductances lie between these bounds.

Limited experimental contact conductance results lie between the bounds in very good agreement with the iterated hardness model.

For limited load ranges the BHM with the appropriate hardness predicts contact conductances in good agreement with some experimental results.

For large  $t/\sigma$  the ITM and INM results are similar, while for small  $t/\sigma$  the ITM and BHM results are also similar.

It is recommended that further experimental results be obtained to verify the validity of the models over a wide range of contact pressure and hardness variation of different materials.

Also it is recommended that further studies be done to determine the effect of different machining processes upon the thickness of the work-hardened layer which in turn influences the thermal conductances.

It is further recommended that a general theory be developed for two rough surfaces each having a different hardness distribution.

#### Acknowledgments

The authors greatly appreciate the financial support of AECL Whiteshell Nuclear Reactor Establishment. The senior author also acknowledges the partial support of the National Science and Engineering Research Council of Canada.

The authors also thank Dr. M.H. Schankula for his contributions to this research and V.W. Antonetti for giving us his data.

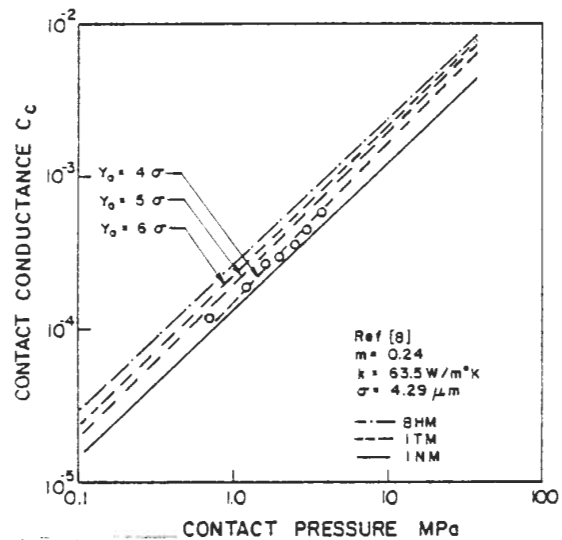


Fig. 16 Comparison between the BHM, ITM, INM and experimental results of Ref. 8.

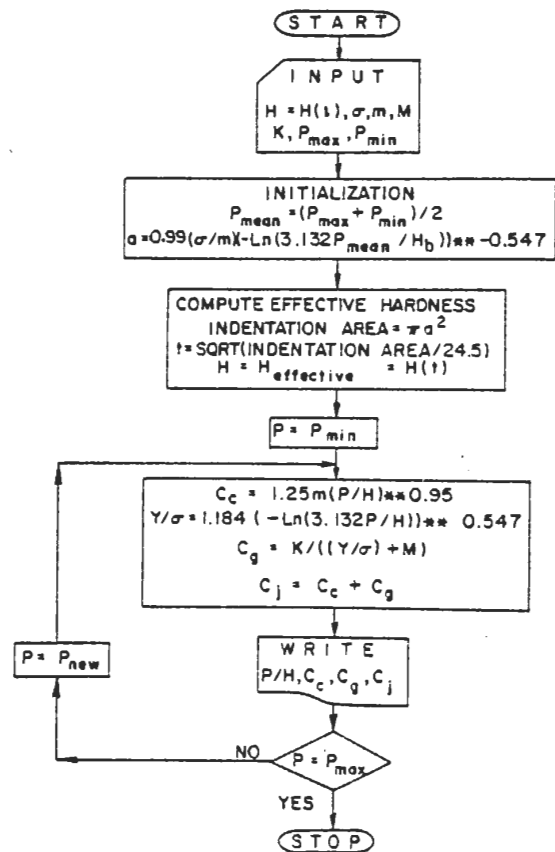


Fig. 17 Direct approximate method solution procedure.



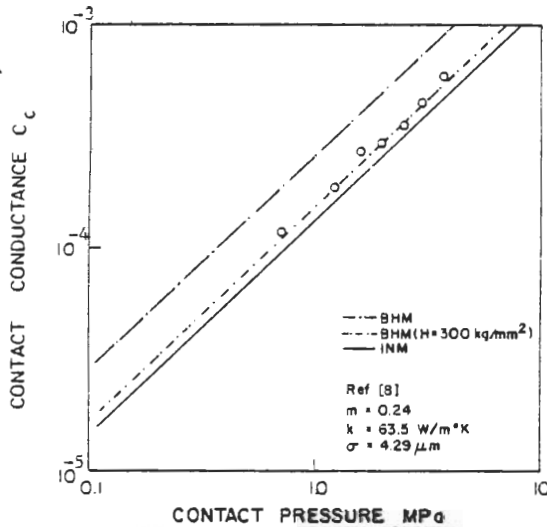


Fig. 18 Comparison between the BHM, INM, direct approximate method and the experiments of Ref. 8.

Table 1: Comparison between ITM and experiments for ζ = 4.0 Ref. 8.

P KN/m <sup>2</sup>	r μm	H kg/mm <sup>2</sup>	10 <sup>4</sup> C <sub>c</sub>	10 <sup>4</sup> C <sub>c</sub> exp	%Diff.
698	2.149	313.8	1.035	1.184	14.42
1194	2.856	290.9	1.852	1.858	0.33
1559	3.211	282.0	2.458	2.670	8.64
1925	3.494	275.7	3.068	2.944	-4.03
2450	3.819	269.2	3.937	3.508	-10.90
2890	4.051	265.1	4.691	4.44	-5.35
3636	4.369	259.8	5.938	5.836	-1.73

Average Hardness = 279.5 kg/mm<sup>2</sup>  
 Sum of % Diff. = 1.38  
 Average of % Diff. = 0.20

### References

- Boeschoten, F. and Van der Held, E.F.M., "The Thermal Conductance of Contacts Between Aluminum and Other Metals", *Physica*, Vol. 23, 1957, pp. 37-44.
- Laming, L.C., "Thermal Conductance of Machined Contacts", 1961 International Heat Transfer Conference, Part 1, No. 8, pp. 65-76, Boulder, Colorado, 1961.
- Mott, M.A., *Micro-Indentation Hardness Testing*, Butterworths Scientific Publications, London, 1956.
- Clausing, A.M. and Chao, B.T., "Thermal Contact Resistance in a Vacuum Environment", University of Illinois, Report ME-TN-242-1, August 1963.
- Henry, J.J., "Thermal Contact Resistance", Ph.D. Thesis, MIT, 1964.
- Kragelskii, I.V., *Friction and Wear*, Butterworths Scientific Publications, London, 1965.
- Greenwood, J.A. and Williamson, J.B.P., "Contact of Nominally Flat Surfaces", *Proc.R.Soc. A295*, pp. 300-319, 1966.
- Antonetti, V.W., Ph.D. Thesis in progress, Department of Mechanical Engineering, University of Waterloo.
- Hegazy, A.H., Ph.D. Thesis in progress, Department of Mechanical Engineering, University of Waterloo.
- Yovanovich, M.M., "New Contact and Gap Conductance Correlations for Conforming Rough Surfaces", AIAA Paper No. 81-1164, AIAA 16th Thermophysics Conference, June 23-25, Palo Alto, CA., 1981.